Iranian Journal of Medical Physics
Vol. 12, No. 1, Winter 2015, 49-61
Received: August 17, 2014; Accepted: February 5, 2015

Original Article

Induction of Localized Hyperthermia by Millisecond Laser Pulses in the Presence of Gold-Gold Sulphide Nanoparticles in a Phantom

Zahra Shahamat[1], Mahin Shokouhi[1], Ahmad- Reza Taheri[2], Hossein Eshghi[3], Neda Attaran-Kakhki[3], Ameneh Sazgarnia[1]*

Abstract

Introduction
Application of near-infrared absorbing nanostructures can induce hyperthermia, in addition to providing more efficient photothermal effects. Gold-gold sulfide (GGS) is considered as one of these nanostructures. This study was performed on a tissue-equivalent optical-thermal phantom to determine the temperature profile in the presence and absence of GGS and millisecond pulses of a near-infrared laser. Moreover, the feasibility of hyperthermia induction was investigated in a simulated tumor.

Materials and Methods
A tumor with its surrounding tissues was simulated in a phantom made of Agarose and Intralipid. The tumor was irradiated by 30 laser pulses with durations of 30, 100, and 400 ms and fluences of 40 and 60 J/cm^2. Temperature variations in the phantom with and without GGS were recorded, using fast-response sensors of a digital thermometer, placed at different distances from the central axis at three depths. The temperature rise was recorded by varying duration and fluence of the laser pulses.

Results
The rise in temperature was recorded by increasing laser fluence and number of pulses for three durations. The temperature profile was obtained at each depth. The presence of GGS resulted in a significant increase in temperature in all cases ($P<0.035$). Also, the laser temperature had a slower reduction in the presence of GGS, compared to its absence after turning the laser off ($P<0.001$).

Conclusion
The millisecond laser pulses could induce hyperthermia in a relatively large target tissue volume. GGS as a simple and cost-effective synthesized nanostructure could induce localized hyperthermia in the desired region during near-infrared laser irradiation.

Keywords: Hyperthermia; Photothermal Therapy; Pulse Duration; Gold-Gold Sulfide; NIR Laser.

1- Medical physics Dept., Research Center of Medical Physics, Mashhad University of Medical Sciences, Mashhad, Iran
*Corresponding author: Tel: +98 513 8002323, Fax:+98 513 8002320; E-mail: sazgarniaa@mums.ac.ir

2- Cutaneous Leishmaniasis Research Center, Department of Dermatology, Mashhad University of Medical Sciences, Mashhad, Iran
3- Department of Chemistry, Faculty of Sciences, Ferdowsi University of Mashhad, Mashhad, Iran

1. Introduction

When the tissue temperature exceeds 40 °C, blood flow increases in both tumoral and normal tissues [1, 2]. Cellular cytotoxicity might occur as the temperature reaches 41.5 °C [3]. In fact, temperatures above 42.5 °C can result in vascular destruction within tumoral tissues [4]. Thermal impact on tissues drastically alters when temperature exceeds 43 °C. Moreover, the rate of "cell killing" doubles for every 1 °C increase beyond 43 °C and decreases by a factor of 4-6 for every 1 °C drop below 43°C [5, 6].

Tumoral tissues have been shown to be more sensitive to temperature rise, compared to normal tissues [7]. An important reason for the observed cytotoxicity, associated with temperature rise, is that thermal effects are more profound in acidotic conditions (low pH) in poorly oxygenated human tumors. Consequently, heat has a greater cytotoxic effect on tumors, compared to normal tissues [3]. However, heat alone only has limited effects and the observed thermal impacts are limited to short durations, which are applied in cancer treatment [8, 9]. Furthermore, when heat is applied, damage to the surrounding tissues is often inevitable.

Lasers with precise energy-delivery mechanisms can be effective instruments for the photothermal treatment of cancer. However, selectivity has been a major challenge in non-invasive treatment of deep tumors. Absorption of laser energy by a tissue depends on light wavelength and the optical properties of the tissue. Strong absorption can cause thermal injuries mainly to the surface tissues, which are being treated, and in turn will limit the scope of thermal effects on deeper tissues. However, weak absorption by a tissue does not suffciently raise the tissue temperature.

One of the ways to improve the laser heating spatial selectivity is tumor photothermal labeling by gold nanoparticles (NPs) with different shapes and structures such as nanoshells [10, 11], nanorods [12, 13], nanocages [14], and others. Researchers have recently started to engineer multifunctional NPs with properties suitable for both imaging and treating cancer in order to manage and treat the disease more efficiently.

Gold-gold sulfide (GGS) NPs can act as a dual contrast and therapeutic agent when combined with two-photon microscopy [15]. These NPs strongly absorb near-infrared (NIR) wavelengths of light, which deeply penetrate into tissues [16]. Their application is useful for NIR photothermal therapy and optical imaging. Several gold-based NIR-absorbing NPs, e.g., silica-gold nanoshells [17, 18], gold nanorods [12, 13], and gold nanocages [14] have exhibited the ability to convert incident light energy into adequate heat in order to irreversibly damage the target cancerous cells.

Therefore, GGS may be utilized to perform NP-assisted photothermal therapy as an adjuvant modality, in association with conventional treatments. GGS is anticipated to provide a minimally invasive and highly effective method with limited side-effects. Furthermore, GGS nanoshells are biocompatible, capable of targeting cancerous cells, and are selectively absorbed by target cells.

Compared to gold nanoshells with a silicone core, GGSs are synthesized with a smaller diameter and their absorption peak is in the NIR region. Additionally, considering their broad absorption band, non-laser light sources may be used in photothermal therapy in order to induce hyperthermia; however, the simple and inexpensive synthesis of nanoshells should not be ignored. On the other hand, the possibility to trace NPs prior to treatment can prevent the untargeted delivery of heat to healthy tissues by inducing a thermal contrast between normal and damaged tissues [15].

In this study, temperature variations of a simulated tumor were recorded during NIR laser irradiation at 12 different positions in order to predict the feasibility of inducing hyperthermia by millisecond laser pulses and determine the temperature difference between the tumor (with GGS) and its surrounding tissues (without GGS). Also, the effects of

pulse duration and fluence of laser pulses on the temperature profile were evaluated.

Although previous researchers have used short laser pulses (e.g., nanoseconds or less) to prevent heat leakage into the neighboring tissues, we examined the effect of millisecond pulses, since the extent of the target volume to which hyperthermia is induced is usually larger and millisecond lasers can be acted more effective than nanosecond lasers. Therefore, the main objective of this study was to evaluate the possibility of using GGS rather than gold nanoshells () with a silicon core, along with a long duration of laser pulses, in order to distribute and leak heat into a relatively large target tissue and induce hyperthermia.

The mentioned application of GGS has not been evaluated in previous studies and there are no papers to which we can refer. However, a previous study showed that extinction and scattering coefficients of GGS at NIR region are greater and smaller than GNS, respectively. Obviously, considering the short thermal relaxation time of gold nanostructures, we need to apply short-duration laser pulses for executing photothermal therapy via the photoablation process, mediated for gold nanostructures.

2. Materials and Methods

2.1. GGS-NP synthesis and characterization

GGS-NPs have been synthesized using a variety of procedures, as described by Averitt et al. [19] and Schwartzberg and colleagues [20]. $HAuCl_4$ (2 mM, Alfa Aesar, Ward Hill, MA) and $Na_2S_2O_3$ (1 mM, Sigma, Saint Louis, MO) solutions were prepared in milli-Q water, aged two days at room temperature, and mixed in small quantities at volumetric $HAuCl_4$:$Na_2S_2O_3$ ratios ranging from 1:1 to 1:2.

The ratio that produced an NP resonance near 800 nm, as determined with an ultraviolet (UV)-visible spectrophotometer (Cary 50, Varian, Walnut Creek, CA), was used to synthesize a large batch of NPs for in vitro experiments. After preparing the NPs, polyvinylpyrrolidone was added to prevent GGS aggregation.

The particle size distribution of NPs was determined by a particle size analyzer (Malvern Instruments, USA). Furthermore, we utilized a UV-visible spectrophotometer (UV1700 Shimadzu, Japan) to record the spectrum of UV-visible GGS absorption. Also, an electron microscope (Philips CM120, Germany) was applied and ran at an acceleration voltage of 120 kV to examine GGS morphology.

2.2. Moulds of phantom and simulated tumor

The phantom consisted of two parts. The inner part simulated a tumor (20 mm in height and 9 mm in diameter), and the outer part simulated the surrounding tissues of the tumor. The phantom was prepared into a cylindrical mould (160 mm in diameter and 80 mm in height), made of Teflon. Teflon was selected given the ease of extracting the phantom material and lack of chemical interactions with materials.

In the mould wall, three holes were vertically embedded in four directions parallel to the central axis, with a 45° angle, relative to each other (Figure 1). The diameter of the holes was 2.5 mm and the centers of the adjacent holes in each column stood within a 4.5 mm distance from each other. The main reason for this arrangement was to prevent the effect of each sensor on others due to shadow formation on the next sensor.

A cavity (9mm in diameter) was created in the center of the cylindrical shell, closed by a pin (40 mm in height). To locate the sensors (thermocouple probe Type K, Testo 735-2), four plastic-coated stainless steel pins with the same holes, aligned alongside the center of the mould, were placed in the following arrangement: 1) the first pin in the mould center, 2) the second pin in a 3 mm distance from the center, 3) the third pin tangent to the edge of the simulated tumor (in a 4.5 mm distance from the center), and 4) the fourth pin in a 3mm distance from the edge of the simulated tumor (a 7.5 mm distance from the center).

A cylindrical aluminum mould with an internal diameter of 9 mm and height of 20 mm was made. This mould was designed in order to prepare a tumor-like phantom.

2.3. Preparation of tissue-equivalent phantoms

Gel phantoms were prepared from 1% Agarose and 1% Intralipid™ (10% fat emulsion, Baxter, Toronto, Canada) with GGS evenly dispersed throughout the structure. In brief, 15,600 mg of highly purified Agarose powder (Type VII-A: low gelling temperature, Sigma) was mixed with 1400 ml of double deionized water and heated by a microwave for 2-4 min (at 90 °C) with intermittent stirring until the Agarose was dissolved and the solution appeared clear and colorless.

While being continuously mixed at room temperature, the Agarose solution was permitted to cool down to 60 °C. Simultaneously, 156 ml of Intralipid™ was added, which made the solution whitish in color and opaque. The resulting solution was constantly mixed until cooling down to 45 °C; it was then poured into the mould [21]. GGS (concentration= 5×10^4 mM/ml [21], volume =140µl) was added to the phantom tumor-simulating solution, as its concentration in the tumor was 13.8 mM/ml.

2.4. Irradiation setup

Phantom irradiation was performed by a diode laser system (805nm, Lumenis Ltd., Lumenis One ™ System, Lightsheer); thirty pulses were applied at 1 Hz frequency and pulse widths of 30, 100, and 400 ms; the radiation fluencies were selected as 40 and 60 J/cm^2. The laser pulse parameters are given in Table 1.

Table 1. Specifications of laser pulses in different experiments in phantoms with and without GGS-NPs

Number of pulses	Pulse duration (ms)	Fluence (J/cm^2)	
30	30	40	60
	100	40	60
	400	40	60

Changes in phantom temperature were recorded 5 seconds before irradiation and continued till 200 seconds after the cessation of laser irradiation. The sensors were inserted in 1.5, 9, and 14 mm depths, along the central axis of the cylindrical phantom. The central phantom (the simulated tumor) was then exchanged with the phantom containing NPs and changes in temperature were recorded under the same irradiation. Figures 1a and 1b show the schematic design and experimental setup, used for phantom irradiation.

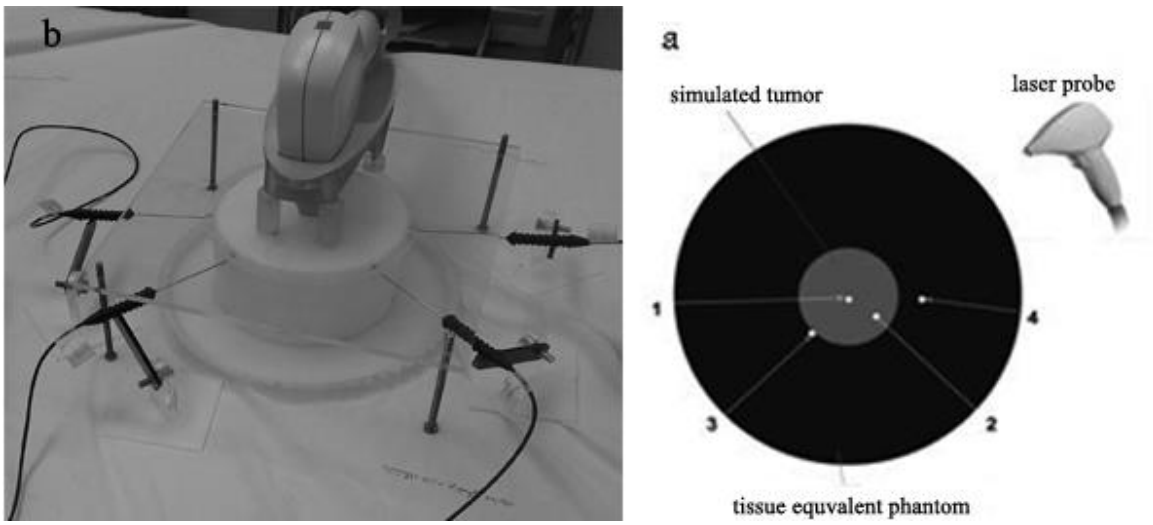

Figure 1a: Schematic design of the experimental setup used for phantom irradiation; numbers 1-4 demonstrate the position of temperature sensors; 1b) the experimental setup used for phantom irradiation and temperature measurement

2.5. Statistical analysis

Statistical analysis was performed on the obtained data. The relationships between phantom depth, pulse duration, and fluence were determined using the generalized linear model. Also, based on Kolmogorov-Smirnov test results, data distribution was normal. Therefore, the effect of each variable on other parameters was assessed separately by Tukey's test.

3. Results

3.1. GGS-NP characterization

Figure 2 shows the absorption spectrum of GGS in water. The wavelengths of absorption peaks were observed at 520 and 820 nm, which was consistent with the synthesis and purification of GGS-NPs. The particle size distribution of NPs is demonstrated in figure 3.

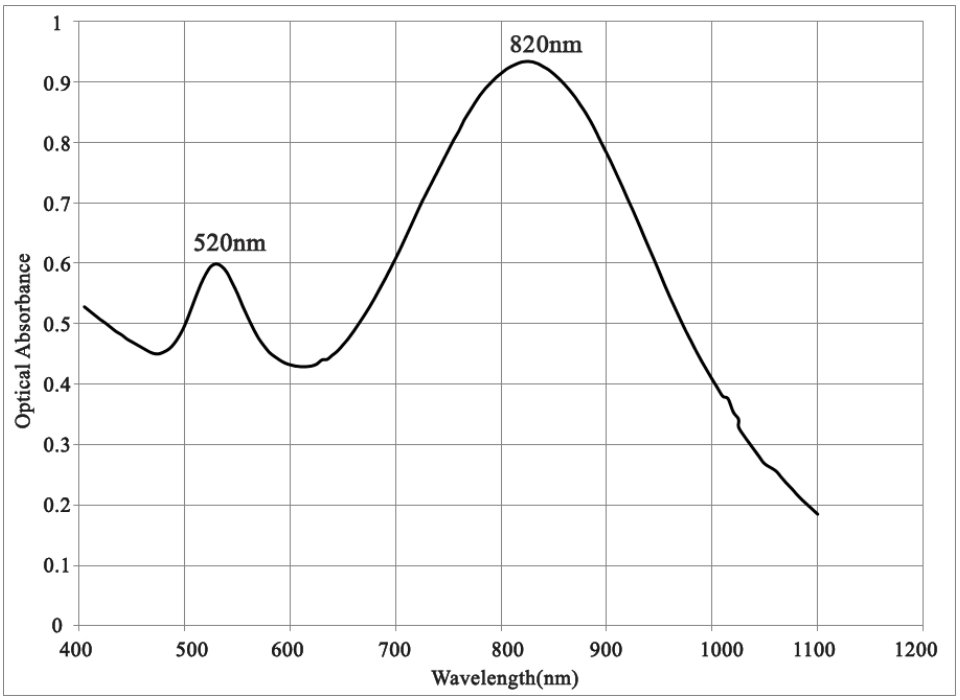

Figure 2. Absorption spectrum of GGS in water

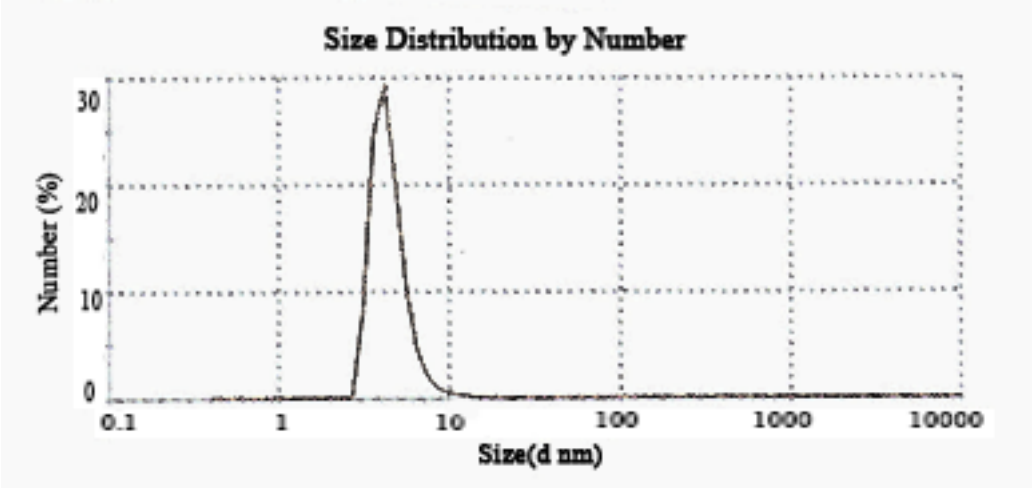

Figure 3. Size distribution of GGS-NPs

3.2. Assessment of changes in phantom temperature

The effects of laser fluence and duration on temperature variations were surveyed at depths of 1.5, 9, and 14 mm in the presence and absence of GGS. As shown in figure 4, the temperature patterns exhibited the same behavior in depths of 1.5 and 9 mm, whereas a different pattern was observed in the depth of 14 mm.

One of the most important observations was the rise in temperature with an increase in pulse fluence (Figure 4). Also, at fluences of 40 and 60 J/cm^2, pulses with a shorter duration caused a more significant increase in temperature ($P<0.046$). Another important finding was the significant increase in temperature in the presence of NPs ($P<0.035$). In other words, in the presence or absence of GGS, for depths of 1.5, 9, and 14 mm, the greatest variations in temperature were induced by 30 pulses with the fluence of 60 J/cm^2 and pulse duration of 30 ms; the lowest amount of variation was obtained using 30 pulses with a 40 J/cm^2 fluence and 400 ms duration.

It must be noted that temperature variations at a 14 mm depth with GGS was less significant than that without GGS. In other words, there was an inverse correlation between temperature variations and presence or absence of GGS in the depth of 14 mm.

3.4. Temperature profile in the simulated tumor

Temperature variations were recorded in the phantom following irradiation by 30 pulses at 30, 100, and 400 ms durations and 40 and 60 J/ cm^2 fluences via inserting 12 points in different phantoms with and without GGS. The recorded data are shown in figures 5 and 6.

3.5. Quality of temperature rise and drop in the simulated tumor

The temperature rise per fluence for each pulse at different durations and depths and temperature drop in the simulated tumor after turning off the laser are presented in figures 7and 8. Based on the obtained data, the required time for temperature descent to 37% of the initial temperature was estimated at 8.6 s in the tumor without GGS and 19.2 s in the tumor with GGS. In other words, the time in the phantom with GGS was more than twice the time without NPs. Thus, it can be stated that temperature variations in the presence of GGS were slower than those reported in the absence of GGS. This finding might be related to the dielectric core or the gradual release of heat energy from NPs.

Based on the penetration depth obtained in this study, GGS can be considered as a suitable candidate for photothermal therapy. GGS synthesis is more simple and cost-effective in comparison with NIR-absorbing nanostructures such as CNT and, GNS and GNP; in addition, it provides a greater treatment depth in relation to GNPs, irradiated by a visible laser. It should be noted that a targeted configuration of GGS-NPs is required to provide enough uptake by the target cells after a low dose administration to the patient.

This study was performed on a tissue-equivalent phantom; however, blood perfusion was ignored. Obviously, blood circulation can be influenced by heat transfer and can lead to faster heat distribution in the irradiated tissue and its surroundings. In this respect, the interval between laser pulses plays a significant role in the quality of temperature rise. Based on a pilot study on a mouse model of colorectal cancer, after tumor irradiation under similar conditions of laser pulses, the recorded temperature rise in the tumor was significantly more significant than that reported in the phantom.

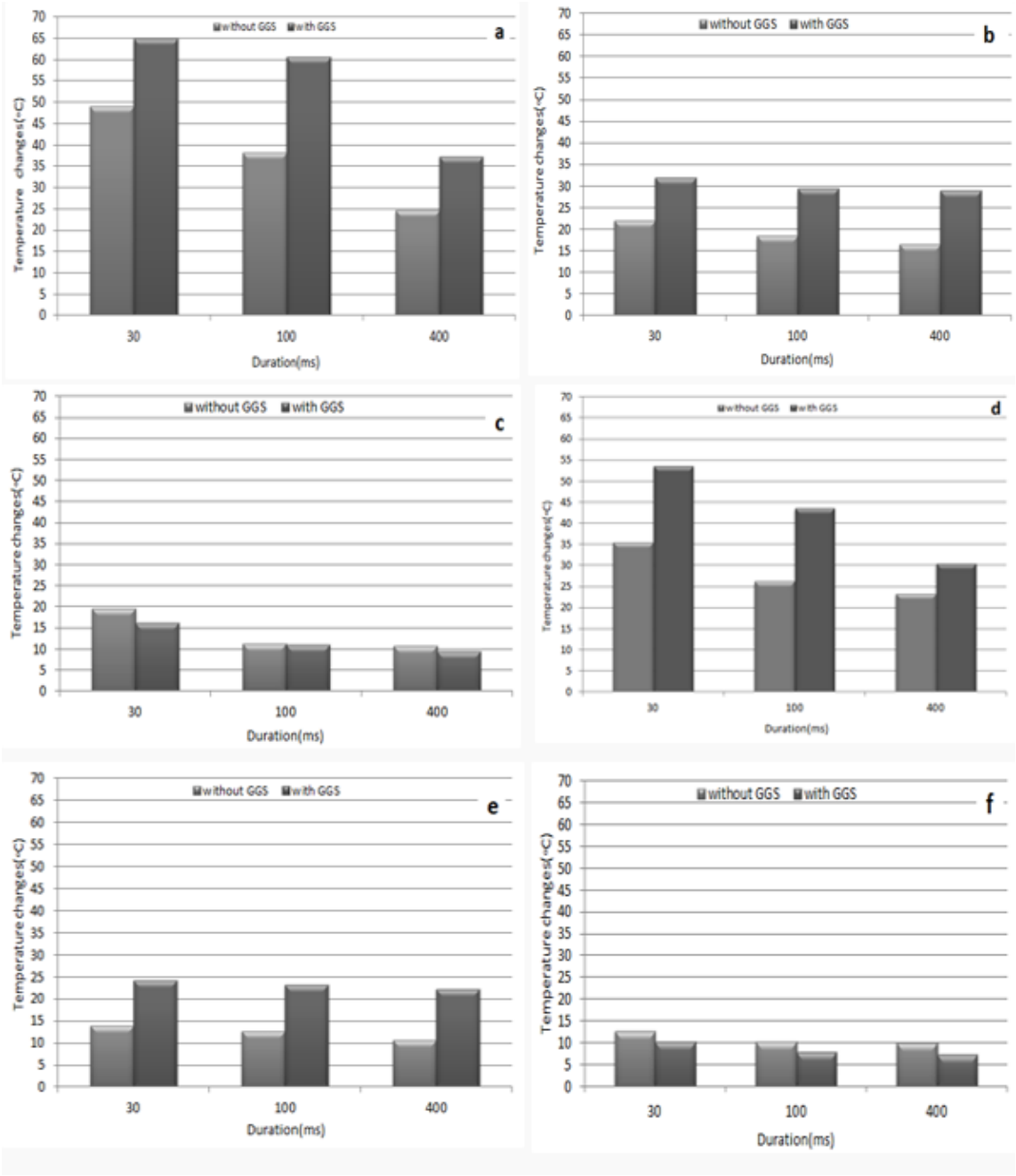

Figure 4. The maximum temperature on the central axis of the phantom in the presence and absence of GGS after irradiation by laser pulses with a fluence of 60 J/cm^2 in depths of a) 1.5 mm, b) 9 mm, and c) 14 mm and fluence of 40J/cm^2 in depths of d) 1.5mm, e) 9mm, and f) 14mm

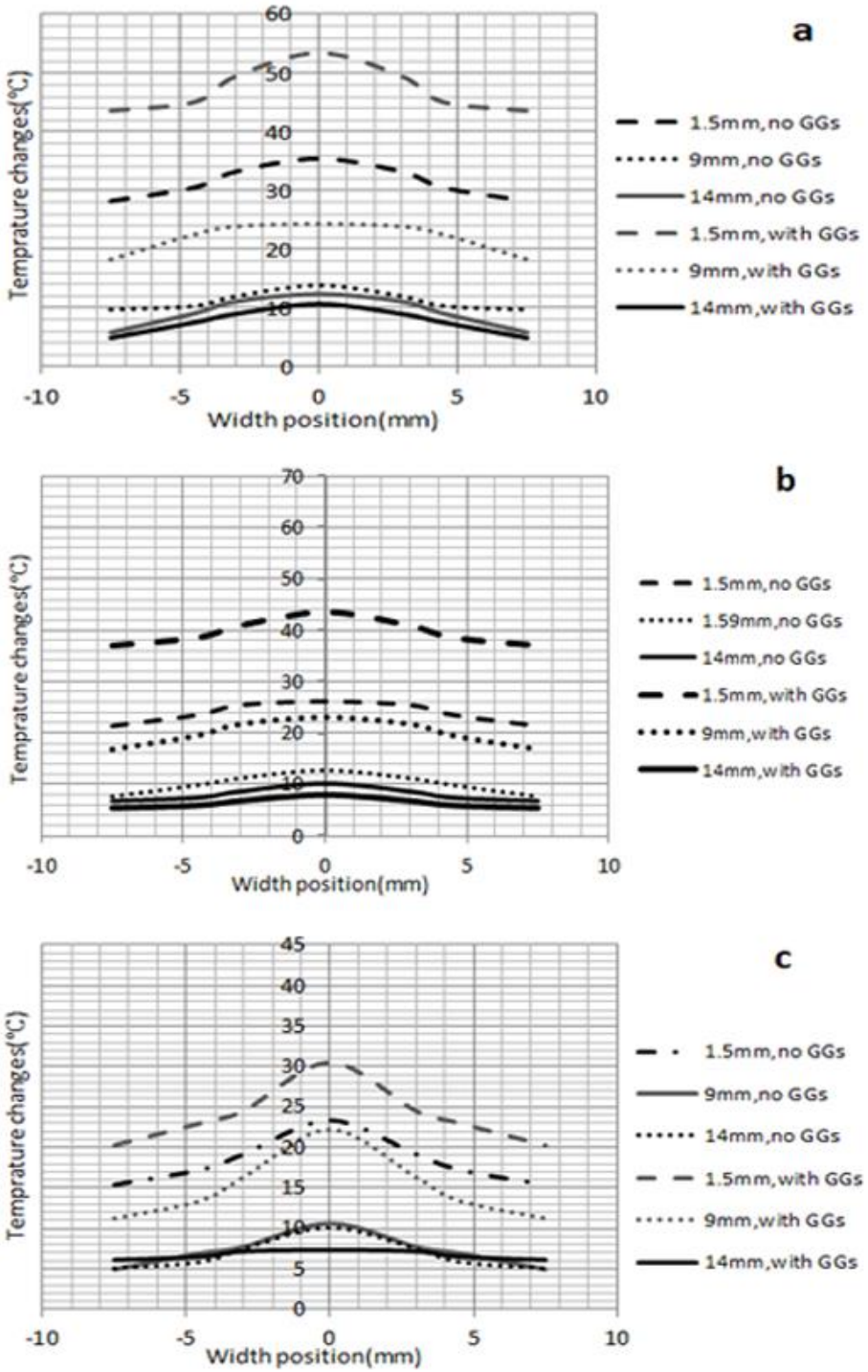

Figure 5. The maximum temperature recorded in the phantom following exposure to 30 laser pulses with a fluence of 40 J/cm^2 in the presence and absence of GGS at pulse durations of a) 30 ms, b) 100 ms, and c) 400 ms

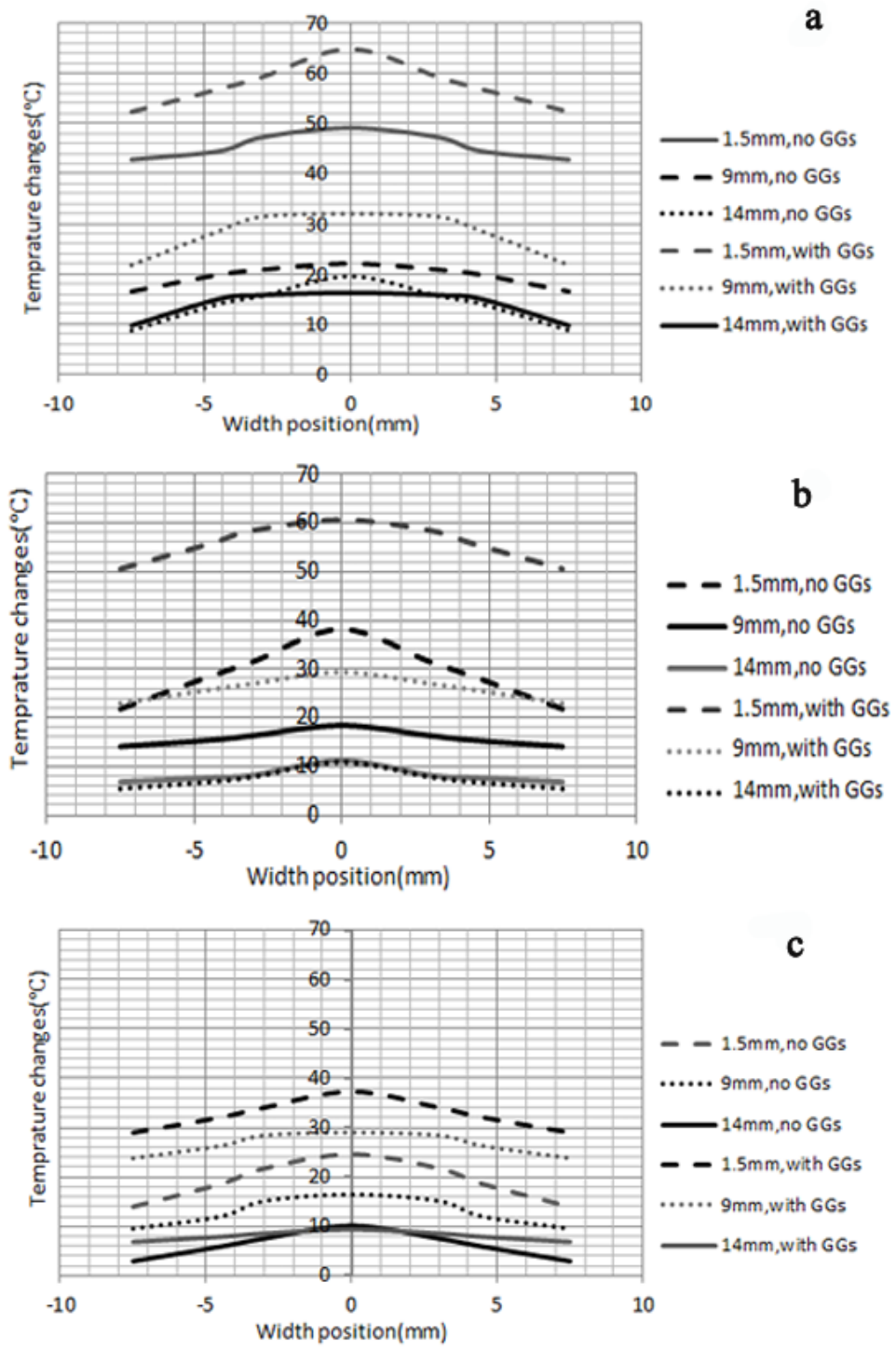

Figure 6. The maximum temperature recorded in the phantom following exposure to 30 laser pulses with a fluence of 60 J/cm^2 in the presence and absence of GGS at pulse durations of a) 30 ms, b) 100 ms, and c) 400 ms

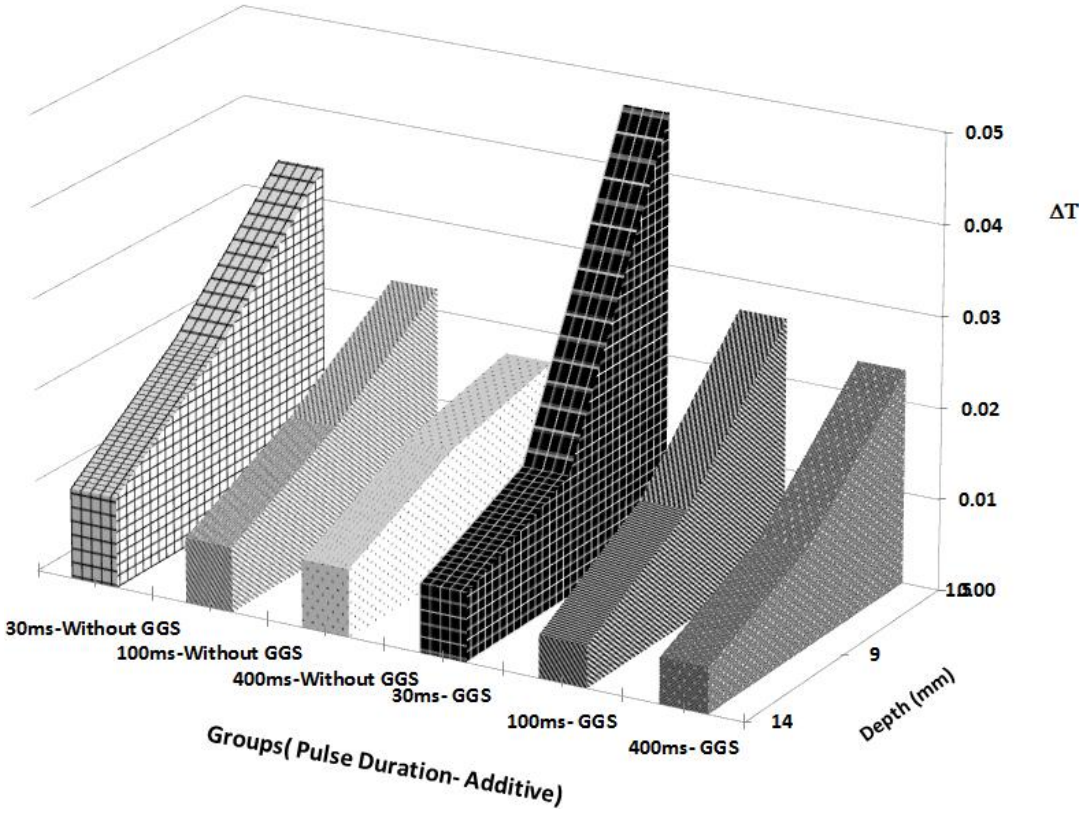

Figure 7. Temperature variations per fluence per pulse at three depths of the simulated tumor during laser irradiation

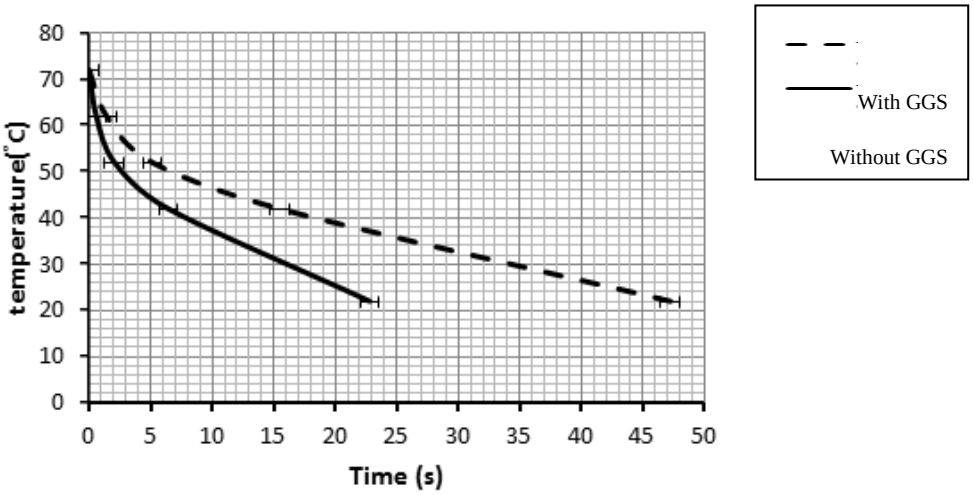

Figure 8. Temperature decline of the phantom after turning off the laser

Based on the penetration depth obtained in this study, GGS can be considered as a suitable candidate for photothermal therapy. GGS synthesis is more simple and cost-effective in comparison with NIR-absorbing nanostructures such as CNT and, GNS and GNP; in addition, it provides a greater treatment depth in relation to GNPs, irradiated by a visible laser. It should be noted that a targeted configuration of GGS-NPs is required to provide enough uptake by the target cells after a low dose administration to the patient.

This study was performed on a tissue-equivalent phantom; however, blood perfusion was ignored. Obviously, blood circulation can be influenced by heat transfer and can lead to faster heat distribution in the irradiated tissue and its surroundings. In this respect, the interval between laser pulses plays a significant role in the quality of temperature rise. Based on a pilot study on a mouse model of colorectal cancer, after tumor irradiation under similar conditions of laser pulses, the recorded temperature rise in the tumor was significantly more significant than that reported in the phantom.

4. Discussion

Currently, the unique properties of NPs in medicine have led to significant developments in various medical fields. In fact, NPs are considered as agents for novel diagnostic and therapeutic applications. Nanoshells and nanotubes are the first potent phototherapeutic agents. Considering the severe surface plasmon resonance of NPs, their intense light absorption in the NIR region can be utilized in photothermal therapy.

In photothermal therapy, two different objectives are considered: 1) induction of hyperthermia by increasing temperature up to 42.5-47 °C in the target tissue for major treatments such as radiotherapy (for creating hyperthermic conditions, laser parameters should be selected considering a low fluence and/or long duration); and 2) induction of ablation which is required for lasers with higher intensities and shorter pulses, compared to what needed for photothermal interactions. These conditions result in the destruction of the target tissue via photoablation and/or plasma-induced ablation as the main therapeutic method.

The main aim of this study was to evaluate the feasibility of the first objective in the presence of GGS. Hyperthermia induced by radiofrequency and NIR accelerates the damage and death of cancerous cells during main treatment modalities. If GGS is irradiated by NIR, photons will be strongly absorbed by the nanoparticles. The physical origin of the absorption is a collective resonant oscillation of the free electrons of the conduction band of the metalic atoms..

During the transmission of light through soft tissues, photon flux is decreased from the surface to the depth of soft tissues, whereas in the presence of GGS and NIR, the resonant incident electric field of the photons can produce subsequent oscillations, which create dipole moments and displacement of the conduction-band electrons. These phenomena in turn convert energy into heat in the targeted tissue.

In this study, first, the absorbance spectrum of GGS-NPs was recorded in the wavelength range of 400-1100 nm. The two absorption peaks were observed at 530 and 820 nm, respectively. The origin of 820 nm peak was the surface plasmon resonance of GGS; the peak around 530 nm belonged to the unreacted $HAuCl_4$. Afterwards, the dependence of phantom temperature on duration and fluence of laser pulses at different depths of the phantom was compared in phantoms containing GGS and those without GGS; moreover, temperature variation profile and temperature drops after the cessation of laser irradiation were investigated.

Obviously, increasing the light power density is possible by increasing the fluence with certain durations or reducing duration with a certain fluence. At a selected radiation period, a certain amount of the transferred energy is deposited on the phantom layers, whereas a

part of it passes through. The absorbed energy increases the local temperature, which will gradually spread in the surrounding tissues. The deposited energy leads to a temperature rise, while transferring energy to the surrounding tissues can reduce the phantom temperature.

By receiving pulses with a shorter duration, the rate of energy transfer will be more than the rate of energy loss; therefore, a greater rise in phantom temperature will occur. If the rate of energy transfer remains constant, while the fluence increases, the rise in temperature will be even greater. These findings were further confirmed by the obtained results at different fluences and pulse durations.

With and without GGS, a rise in temperature was observed in the first (1.5mm) and second (9mm) depths, while in the third depth (14mm), an opposite outcome was reported in the presence of NPs with different durations and fluences. This occurrence may be due to the higher absorption of light photons by GGS-NPS in the upper layers of the phantom, which prevents their receipt by the underlying parts.

The gradual absorption of radiation by GGS particles in the upper layers of the phantom causes a decline in the amount of radiation reaching the lower regions. Practically, this is due to the reduced light penetration depth in the presence of GGS, considering the high probability of photon absorption in the phantom. These findings were consistent with the results obtained by Terentyuk et al. in 2009 [22]. In their study, the continuous absorption of laser radiation by GGS at particle density of $N=5\times10^{9}cm^{-3}$, N/4, N/8, and N/16 was evaluated. The findings suggested that at higher NP concentrations, higher absorption occurs in the superficial layers, whereas with the possible reduction of light absorption in the phantom at lower concentrations, more photons can be received by the lower layers [22].

Indeed, the most important limitation of photothermal therapy with GNPs is the low penetration depth of 520-540 nm wavelengths, which is expected to increase by utilizing NIR with GGS. On the other hand, considering the results of this research, the use of GGS-NPs decreases the penetration depth of NIR. Therefore, the true therapeutic depth in photothermal therapy in the presence of GGS will be less than what is expected from NIR.

5. Conclusion

Hyperthermia induction in a target tissue was feasible in the presence of GGS with irradiation by NIR laser pulses at long durations and low fluences. Based on the findings of this study, it can be concluded that in a tissue-equivalent phantom, involving a simulated tumor, temperature rise decreases from the upper to lower layers during NIR irradiation in the presence of GGS.

Acknowledgements

The authors would like to thank the Research Deputy of Mashhad University of Medical Sciences for the financial support of the study. We also wish to thank Ms. Fathi for her sincere cooperation in the application of laser pulses. This paper was extracted from an M.Sc. thesis of medical physics.

References

1. Reinhold HS, Endrich B. Tumour microcirculation as a target for hyperthermia. Int J Hyperthermia. 1986;2(2):111-37.
2. Song CW, Lokshina A, Rhee JG, Patten M, Levitt SH. Implication of blood flow in hyperthermic treatment of tumors. Biomedical Engineering, IEEE Transactions on. 1984(1):9-16.
3. Thistlethwaite AJ, Leeper DB, Moylan III DJ, Nerlinger RE. pH distribution in human tumors. Int J Radiat Oncol Biol Phys. 1985;11(9):1647-52.
4. Dewey W, Hopwood L, Sapareto S, Gerweck L. Cellular responses to combinations of hyperthermia and radiation. Radiology. 1977;123(2):463-74.

5. Field S, Morris C. The relationship between heating time and temperature: its relevance to clinical hyperthermia. Radiother Oncol. 1983;1(2):179-86.
6. Sapareto SA, Dewey WC. Thermal dose determination in cancer therapy. Int J Radiat Oncol Biol Phys. 1984;10(6):787-800.
7. Hynynen K, Lulu B. Hyperthermia in cancer treatment. Invest Radiol. 1990;25(7):824-34.
8. Dewhirst MW, Conner W, Moon TE, Roth HB. Response of spontaneous animal tumors to heat and/or radiation: preliminary results of a phase III trial. J Natl Cancer Inst. 1982;61:395-7.
9. Marmor JB, Pounds D, Postic TB, Hahn GM. Treatment of superficial human neoplasms by local hyperthermia induced by ultrasound. Cancer. 1979;43(1):188-97.
10. Hirsch LR, Stafford R, Bankson J, Sershen S, Rivera B, Price R, et al. Nanoshell-mediated near-infrared thermal therapy of tumors under magnetic resonance guidance. Proceedings of the National Academy of Sciences. 2003;100(23):13549-54.
11. Maksimova IL, Akchurin GG, Khlebtsov BN, Terentyuk GS, Akchurin GG, Ermolaev IA, et al. Near-infrared laser photothermal therapy of cancer by using gold nanoparticles: Computer simulations and experiment. Medical Laser Application. 2007;22(3):199-206.
12. Dickerson EB, Dreaden EC, Huang X, El-Sayed IH, Chu H, Pushpanketh S, et al. Gold nanorod assisted near-infrared plasmonic photothermal therapy (PPTT) of squamous cell carcinoma in mice. Cancer letters. 2008;269(1):57-66.
13. Huang X, El-Sayed IH, Qian W, El-Sayed MA. Cancer cell imaging and photothermal therapy in the near-infrared region by using gold nanorods. J Am Chem Soc. 2006;128(6):2115-20.
14. Chen J, Wang D, Xi J, Au L, Siekkinen A, Warsen A, et al. Immuno gold nanocages with tailored optical properties for targeted photothermal destruction of cancer cells. Nano Letters. 2007;7(5):1318-22.
15. Day ES, Bickford LR, Slater JH, Riggall NS, Drezek RA, West JL. Antibody-conjugated gold-gold sulfide nanoparticles as multifunctional agents for imaging and therapy of breast cancer. Int J Nanomedicine. 2010;5:445-54.
16. Weissleder R. A clearer vision for in vivo imaging. Nat Biotechnol. 2001;19(4):316-7.
17. Gobin AM, Lee MH, Halas NJ, James WD, Drezek RA, West JL. Near-infrared resonant nanoshells for combined optical imaging and photothermal cancer therapy. Nano Letters. 2007;7(7):1929-34.
18. O'Neal DP, Hirsch LR, Halas NJ, Payne JD, West JL. Photo-thermal tumor ablation in mice using near infrared-absorbing nanoparticles. Cancer letters. 2004;209(2):171-6.
19. Averitt RD, Westcott SL, Halas NJ. Linear optical properties of gold nanoshells. JOSA B. 1999;16(10):1824-32.
20. Schwartzberg A, Grant C, Van Buuren T, Zhang J. Reduction of HAuCl4 by Na2S revisited: the case for Au nanoparticle aggregates and against Au2S/Au core/shell particles. The Journal of Physical Chemistry C. 2007;111(25):8892-901.
21. Didychuk CL, Ephrat P, Chamson-Reig A, Jacques SL, Carson JJ . Depth of photothermal conversion of gold nanorods embedded in a tissue-like phantom. Nanotechnology. 2009; 20(19):195102.
22. Terentyuk GS, Maslyakova GN, Suleymanova LV, Khlebtsov NG, Khlebtsov BN, Akchurin GG, et al. Laser-induced tissue hyperthermia mediated by gold nanoparticles: toward cancer phototherapy. J Biomed Opt. 2009;14(2):021016--9.